Chem. Pap.
DOI 10.1007/s11696-017-0183-y

ORIGINAL PAPER

Investigation of environmental and concentration effects on fluorescence properties of AlQ_3 using mesoporous silica and polyacrylate

Jalal Poostforooshan[1,3] · Alireza Badiei[1] · Gholamali Farzi[2] · Hassan Goldooz[1] · Alfred P. Weber[3]

Received: 8 December 2016 / Accepted: 26 April 2017

Abstract In this work, for the first time, control over the position of maximum emission peak for fluorophore, using embedded tris(8-hydroxyquinoline) aluminum (AlQ_3) complexes into different types of host materials, can be achieved. Moreover, the environmental and concentration effects on luminescent properties were studied. In this regard, different concentrations of AlQ_3 were embedded into the poly(methyl methacrylate-*co*-butyl acrylate) (PMMA-*co*-PBuA) nanoparticles as organic host materials by emulsion polymerization. It is established that the dilution of AlQ_3 in the polymer matrix leads to blue-shift of the luminescence maximum up to 0.32 eV compared to pure AlQ_3. Moreover, AlQ_3 was embedded in SBA-15 type mesoporous silica as an inorganic host material by physical adsorption. Finally, this functionalized mesoporous silica was incorporated into PMMA-*co*-PBuA transparent matrix by blending method to obtain Co-Poly-AlQ_3-SBA-15 as organic–inorganic composite material. It was found that there is no significant wavelength shift on the maximum emission peak of the organic–inorganic composite at various concentrations of AlQ_3-SBA-15. The prepared materials were characterized by powder X-ray diffraction (XRD), N_2 adsorption–desorption, NMR, Fourier transform infrared (FT-IR), dynamic light scattering (DLS), scanning electron microscopy (SEM) and fluorescence spectra.

✉ Alireza Badiei
abadiei@khayam.ut.ac.ir

[1] School of Chemistry, College of Science, University of Tehran, Tehran 14155-6455, Iran

[2] Department of Material and Polymer Engineering, Faculty of Engineering, Hakim Sabzevari University, Sabzevar, Iran

[3] Institute of Particle Technology, Technical University of Clausthal, 38678 Clausthal-Zellerfeld, Germany

Keywords Mesoporous silica · Polymer · Organic–inorganic composite · AlQ_3 · Fluorescence

Introduction

Mesoporous silica/polymer composites have been attracting strong interests in recent years due to their unique properties that are different from the individual components. These materials combine the respective characteristic of polymers and mesoporous silica (Wei et al. 2010; Zhang et al. 2010; Kruk et al. 2008). The special properties of organic polymers are high flexibility, versatility in the design of functional groups, film forming property, easy shaping and ability to control the electrical and optical properties (Zou et al. 2008; Poostforooshan et al. 2014; Shaban et al. 2016). Mesoporous silica materials have also attracted much attention due to their high surface area, suitable channel size, ease for functionalization of nanochannels, high porosity, gas barrier properties, high dye dispersion and optical transparency in visible to UV range (Poostforooshan et al. 2016; Hoffmann et al. 2006; Park et al. 2005; Scott et al. 2001).

In recent years some studies have focused on the preparation and characterization of these kinds of composites that exhibit fluorescent properties (Du et al. 2010; Li and Yan 2009). These composites display good photoluminescence, and the environmental and concentration effects can also influence the maximum emission wavelengths of the resulting composites.

To study the environmental effects on fluorophore, a probe molecule is needed that exhibits different fluorescence peak wavelengths depending on the properties of the surrounding media and concentration. In this regard, different 8-hydroxyquinoline metal derivatives

Published online: 05 May 2017

have been investigated (Karimi et al. 2015a, b). Among the metal complexes, the environmentally sensitive fluorophore tris(8-hydroxyquinoline) aluminum (AlQ_3) has attracted much attention due to its spectral sensitivity (Cölle and Brütting 2004). Furthermore, AlQ_3 is capable to modify organic (Meyers and Weck 2003) and inorganic materials (Wang et al. 2006a) and displaying significant fluorescence in both media. The stability of AlQ_3 in a broad range of media made it a successful and powerful molecular probe to study different environments. AlQ_3 is also becoming the subject of intense interest because it offers a vast range of potential applications in low-voltage OLED design which include easy synthesis, relative stability, good electron transport, and emitting properties (Tang and VanSlyke 1987; Lee et al. 2008; Antony et al. 1999). It was found that aggregation of fluorophores such as AlQ_3 can influence the fluorescent peak wavelength (Li et al. 2006). Consequently, small changes in fluorophore surrounding can lead to large shifts in the fluorescence maximum.

Moreover, AlQ_3 complexes, as optically active materials, should be immobilized in a solid support or embedded in a soft matter matrix from the viewpoint of their potential applications in the nanotechnology field, such as in photovoltaic devices, waveguiding, photodetection and sensing. Among the various matrices, polymers are suitable materials for optic devices, since they are cheap, can be transparent, flexible, and easily processed.

In this work, for the first time, the control over the position of maximum emission peak for fluorophore can be achieved using embedded AlQ_3 complexes into different types of host materials including poly(methyl methacrylate-*co*-butyl acrylate) (PMMA-*co*-PBuA) nanoparticles and mesoporous silica as organic and inorganic hosts, respectively, and assembly of AlQ_3-functionalized mesoporous silica materials in polymer matrix as organic–inorganic composite materials.

Experimental

Materials

Pluronic P123 with composition $EO_{20}PO_{70}EO_{20}$ and average molecular weight of 5800 was purchased from Aldrich. Tetraethyl orthosilicate (TEOS), the silica source, 8-hydroxyquinoline (8-HQ), methyl methacrylate (MMA), butyl acrylate (BuA), $K_2S_2O_8$ (KPS) and sodium dodecyl sulfate (SDS) were purchased from Merck. All of the other reagents and solvents were of analytical reagent grade and used without further purification.

Synthesis of tris(8-hydroxyquinoline) aluminum (AlQ_3)

AlQ_3 was prepared according to the literature (Nakamoto and Ohkaku 1971; Badiei and Goldooz 2012). In a typical synthesis $AlCl_3$ (0.01 mol) was added to the ethanol solution (100 ml) of 8-HQ (0.03 mol) and triethylamine (0.03 mol) under stirring at room temperature overnight. The precipitates were centrifuged and washed with ethanol for several times to obtain yellowish-green AlQ_3 powder.

^{1}H NMR (DMSO, 500 MHz): 8.86 (1H, dd, $J_1 = 4.7$ Hz, $J_2 = 1.2$ Hz), 8.82 (1H, dd, $J_1 = 4.7$ Hz, $J_2 = 1.2$ Hz), 8.30 (1H, dd, $J_1 = 8.4$ Hz, $J_2 = 1.2$ Hz), 8.22 (2H, t, J = 6.8 Hz), 7.53–7.49 (3H, m), 7.44 (1H, dd, $J_1 = 8.3$ Hz, $J_2 = 4.7$ Hz), 7.36 (1H, dd, $J_1 = 8.3$ Hz, $J_2 = 4.7$ Hz), 7.23 (1H, d, J = 4.2 Hz), 7.18 (1H, dd, $J_1 = 8.3$ Hz, $J_2 = 4.7$ Hz) 7.13–7.06 (6H, m). The ^{1}H NMR spectrum of AlQ_3 is shown Fig. 1.

Synthesis and AlQ_3 functionalization of mesoporous silica SBA-15

SBA-15 type mesoporous silica was synthesized using TEOS as silica precursor, Pluronic P123 as a structure directing agent, and HCl to make the media acidic, according to the literature (Hashemi et al. 2009; Shahbazi et al. 2011). The surface functionalization of SBA-15 with AlQ_3 was conducted by soaking the dried SBA-15 in the chloroform solution of AlQ_3 complex at room temperature for 12 h. Briefly, 1 g SBA-15 was suspended in 60 ml of chloroform and an excess amount of AlQ_3 complex was added to the above solution at ambient temperature. The resulting AlQ_3-SBA-15 solid was collected by centrifugation and washed with chloroform for several times.

Synthesis of PMMA-*co*-PBuA and AlQ_3-PMMA-*co*-PBuA nanoparticles

Conventional emulsion polymerization has been chosen to synthesize PMMA-*co*-PBuA nanoparticles. The polymerization was carried out in a three-neck flask with a condenser containing water (85 ml), MMA (7.5 g), BuA (7.5 g), SDS (0.7 g) and $K_2S_2O_8$ (0.08 g). The polymerization reaction was carried out under continuous stirring for 5 h in N_2 atmosphere at 75 °C. After that, the obtained solution was a milky emulsion. The average particle size of the resulting PMMA-*co*-PBuA nanoparticle was 48 nm measured with dynamic light scattering (DLS).

The AlQ_3-PMMA-*co*-PBuA composite nanoparticles were prepared by adding different weight percent (0.01, 0.1, 1 wt%) of AlQ_3 to MMA and BuA monomers through ultrasonic vibration followed by emulsion polymerization.

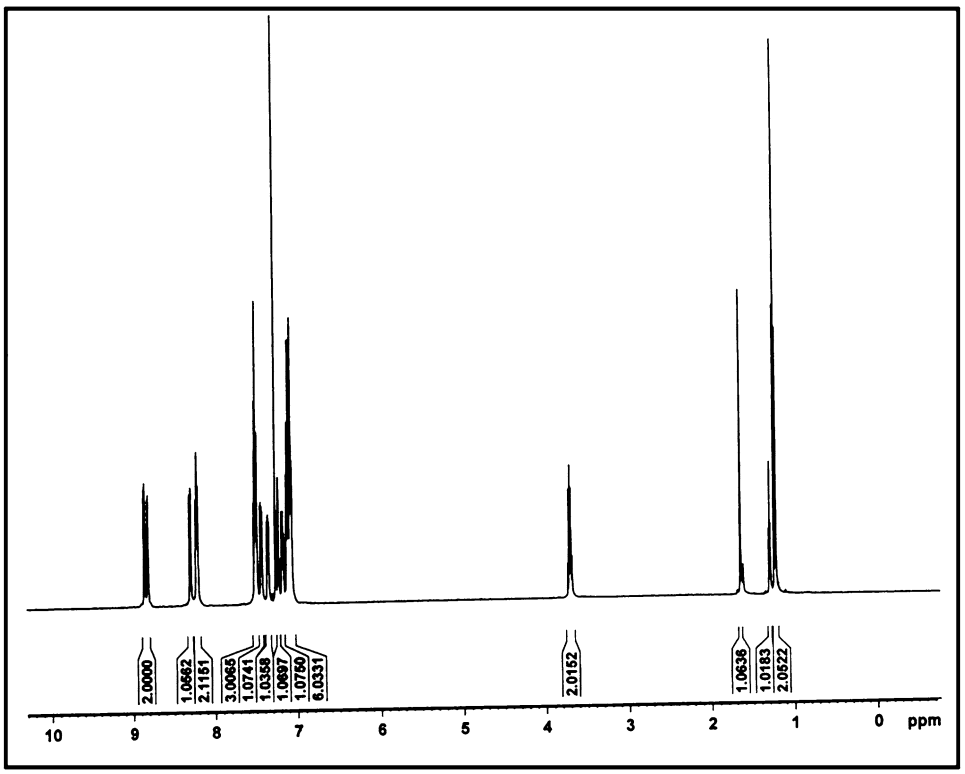

Fig. 1 ^{1}H NMR spectrum of AlQ_3

Preparation of AlQ_3-functionalized mesoporous silica/polymer composites (Co-Poly-AlQ_3-SBA-15)

AlQ_3-SBA-15 was introduced into the PMMA-*co*-PBuA matrix by a blending method. Various concentrations (0.01, 0.1, 1 wt%) of AlQ_3-SBA-15 were dispersed in PMMA-*co*-PBuA matrix under ultrasonic vibration. The transparent composite polymer film was made by casting of the mixture on a clean glass slid and evaporation of the solvent.

Characterization

Small-angle X-ray scattering (SAXS) patterns were recorded with a Philips X′Pert MPD diffractometer using Cu Kα. radiation (40 kV, 40 mA) at a step width of 0.02°. N_2 adsorption–desorption isotherms were measured using a BELSORP mini-II. FT-IR spectra were recorded within a 4000–400 cm^{-1} region on a Bruker Vector 22 infrared spectrophotometer. SEM analysis was performed on a Philips XL-30 field-emission scanning electron microscope operated at 16 kV. ^{1}H NMR of AlQ_3 was performed by using a Bruker spectrometer operating at 500 MHz. The solvent is DMSO. The emission spectra of different samples were recorded by Perkin Elmer LS-50. Particle size analysis of the prepared nanoparticles was carried out by photon correlation spectroscopy (Malvern Zetasizer ZS, Malvern UK).

Results and discussion

Figure 2 shows the SAXS patterns of SBA-15. The sample exhibits a single intensive reflection at the 2θ angle around 0.85° similar to the typical SBA-15 materials, which is generally attributed to the long-range periodicity (Zhao et al. 1998). Two additional peaks corresponding to the

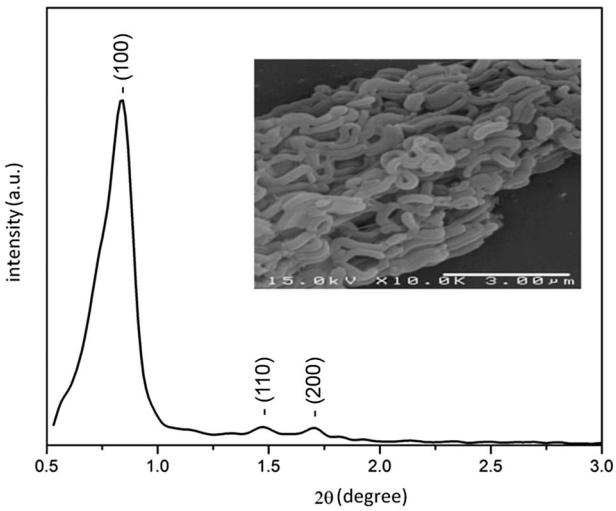

Fig. 2 SAXS patterns for SBA-15. The *inset* is an SEM image of SBA-15

higher ordering (110) and (200) reflections are also observed for the SBA-15 material, that is associated with a two-dimensional hexagonal (*p6 mm*) structure. The inset in Fig. 2 represents an SEM image of SBA-15 which illustrates that the dominant morphologies of particles are short rod-like cylinders. These particles have a diameter of about 400–500 nm and length up to 1 μm, which is typical for SBA-15.

The textural properties of the SBA-15 and AlQ_3-SBA-15 samples were investigated from the nitrogen adsorption–desorption isotherms (Fig. 3). The respective specific surface area (BET method), pore diameter (BJH method) and total pore volume are given in Table 1. The isotherms of these samples present a type-IV isotherm with an obvious H_1-type hysteresis loop which is representative for the mesoporous cylindrical or rod-like channels. These results clearly indicate that the mesostructure is retained during the surface functionalization of SBA-15 with AlQ_3. It should be noted that specific surface area, total pore volume and pore size of SBA-15 were decreased after modification with AlQ_3; indicating that the major functionalization takes place on the surface of the mesopores and full accessibility to the modified nanochannels of SBA-15 is still retained.

Surface modification of SBA-15 with organic functional groups was confirmed by FT-IR spectra (Fig. 4a, b). The

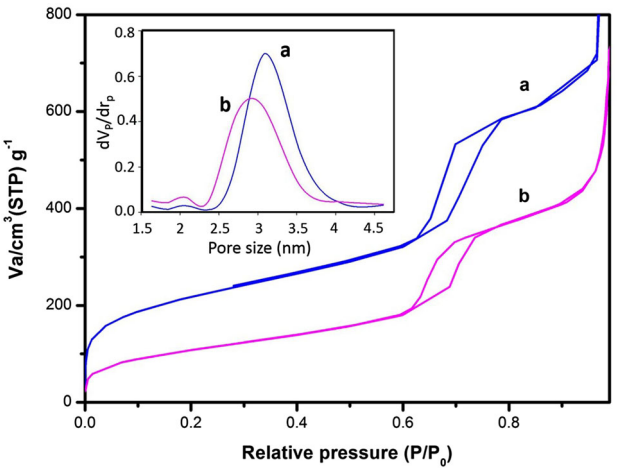

Fig. 3 N_2 adsorption–desorption isotherms of *a* SBA-15, *b* AlQ_3-SBA-15 (*inset* BJH pore size distribution curves of *a* SBA-15, *b* AlQ_3-SBA-15)

Table 1 Textural parameters of prepared compounds

Sample	BET surface area ($m^2\ g^{-1}$)	Total pore volume ($cm^3\ g^{-1}$)	Pore size (nm)
SBA-15	779	1.96	3.1
AlQ_3-SBA-15	388	1.13	2.9

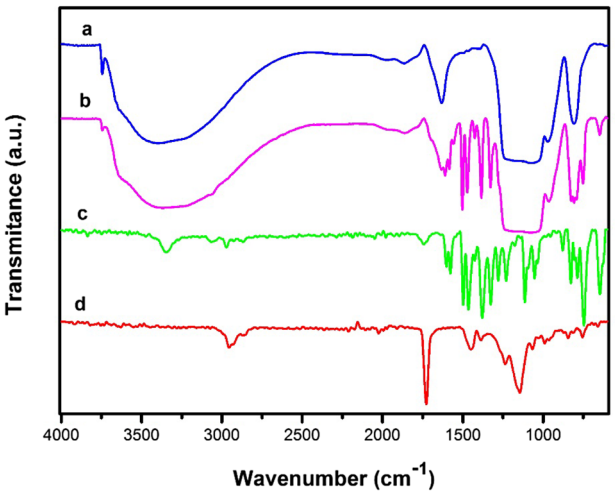

Fig. 4 FT-IR spectra of *a* SBA-15, *b* AlQ_3-SBA-15, *c* AlQ_3 and *d* PMMA-*co*-PBuA

peaks at 1597, 1509, 1471 and 1387 cm^{-1} were related to the C=C and C=N ring skeletal vibrations of an 8-HQ molecule (Nakamoto and Ohkaku 1971; Magee and Gordon 1963; Ganjali et al. 2012). The peak at 646 cm^{-1} could be ascribed to the Al–O stretching modes of the *mer* isomer of AlQ_3 (Curry et al. 2002; Kushto et al. 2000) (Fig. 4b, c). The FT-IR spectrum of PMMA-*co*-PBuA (Fig. 4d) indicates the details of functional groups present in the synthesized PMMA-*co*-PBuA. A sharp intense peak at 1726 cm^{-1} appeared that can be assigned to the presence of ester carbonyl group stretching vibration. The peak at 1145 cm^{-1} can be explained by the C–O (ester bond) stretching vibration. The broad peak ranging from 2900 to 3100 cm^{-1} is due to the presence of C–H group stretching vibration (Balamurugan et al. 2004).

In order to investigate environmental and concentration effects on the fluorescence properties of the AlQ_3, the emission spectra of obtained samples were studied. The photoluminescence (PL) spectra of pure AlQ_3 in chloroform and AlQ_3-loaded PMMA-*co*-PBuA nanoparticles (AlQ_3-poly) with different contents of AlQ_3 are shown in Fig. 5. The positions of maximum emission peak for all samples are listed in Table 2. As a general trend, the PL maximum shifts to higher energies with a dilution of AlQ_3 in the polymer matrix. For the 0.01 wt% sample the corresponding shift is 0.32 eV (60 nm) with respect to a pure AlQ_3 in chloroform. It is clear that any shifting of the fluorescence maximum peak arises from AlQ_3 experiencing a different media. It is assumed that, with the decrease of AlQ_3 concentration, the media electronic properties change and AlQ_3 finds itself in a different environment compared to the bulk. It has been reported that blue-shift in AlQ_3 emission peak is observed by several methods, including modification of ligands (Badiei et al. 2011),

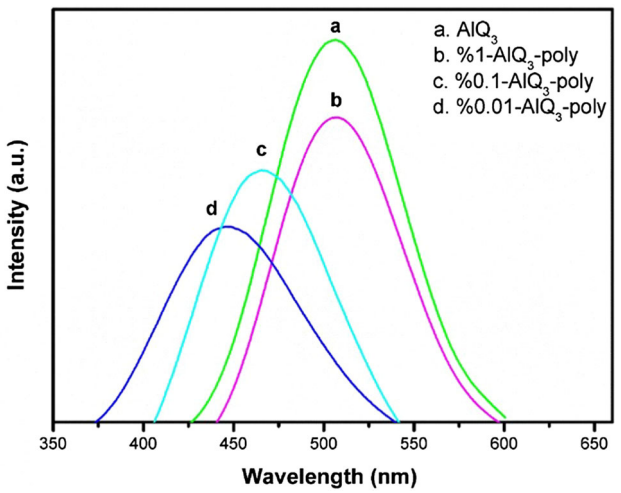

Fig. 5 Fluorescence emission spectra of AlQ_3-PMMA-*co*-PBuA nanoparticles at various concentrations of AlQ_3

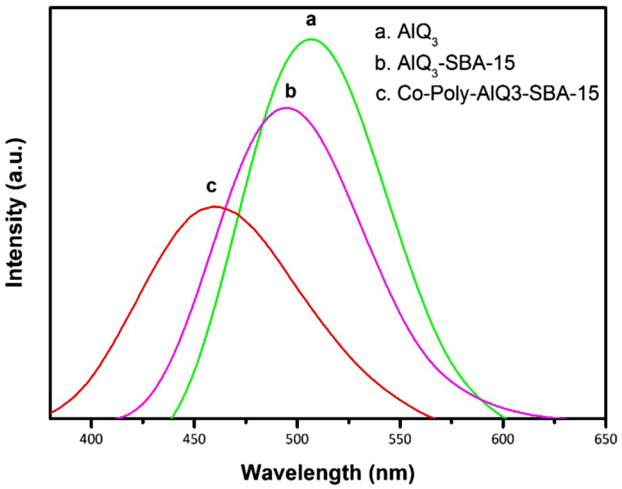

Fig. 6 Emission spectra of *a* AlQ_3, *b* AlQ_3-SBA-15, and *c* Co-Poly-AlQ_3-SBA-15

thermal sublimation in horizontal glass tube (Braun et al. 2001), thin films of AlQ_3 embedded in SiO_2 at low concentration (Levichkova et al. 2006), annealing process (Cölle et al. 2003) or by quantum confinement (Wang et al. 2006b). It should be noted that in this situation, neither annealing nor sublimation at high temperature was done, and yet the maximum emission peak shifts to shorter wavelengths in the fluorescence spectra with a decrease in concentration of AlQ_3 in the polymer matrix. Dhoble and co-workers recently suggested that this blue-shifted behavior can be attributed to cross-relaxation between interacting AlQ_3 molecules (Mahakhode et al. 2011). It was found that there are several energy levels for various phases of AlQ_3 (Brinkmann et al. 2000). Generally, at low concentrations, AlQ_3 complexes are isolated into matrix and emission peak was observed from higher states. As a result, when the concentration reaches the higher level, AlQ_3 molecules come closer and the interaction between them gets increased and excited states may be lowered by cross-relaxation. For that reason, the emission wavelength becomes longer corresponding to these lower excited states. Auzel et al. also reported that the blue-shifts in case of AlQ_3 films seem to be related to the intrinsic properties of the AlQ_3 molecules and its aggregation states rather than Rayleigh scattering (RS) effects on the crystallites of the same film (Auzel et al. 2006). In addition to concentration, the reduced polarity of the environment can cause a blue-shift of emission bands (Bradley et al. 2002; Wang et al. 2011a, b). Since AlQ_3 complexes with low concentration are embedded into the PMMA-*co*-PBuA matrix, the weaker polarity of the environment (the dielectric constant of PMMA-*co*-PBuA is less than 4.8, lower than that of chloroform) (Bradley et al. 2002; Deshmukh et al. 2012) around AlQ_3 led to the blue-shift of the emission band.

Figure 6 shows the PL spectra of AlQ_3 complex in chloroform, AlQ_3-SBA-15 and Co-Poly-AlQ_3-SBA-15, and the maximum emission wavelengths of these materials are summarized in Table 3. AlQ_3 is a yellowish-green powder with a PL maximum at 507 nm. After loading on SBA-15, there is a blue-shift of about 12 nm. Due to the nanometer pore size of mesoporous silica materials, it is difficult for AlQ_3 complexes to aggregate in the nanochannels of SBA-15; therefore, AlQ_3 complexes should be highly dispersed and be present as monomers. Consequently, the mutual distance between AlQ_3 molecules in solution compared with that of AlQ_3-SBA-15, will decrease and then the molecular interaction of AlQ_3 molecules in solution is enhanced. The interaction can result in the spacing of the excited states of AlQ_3 complexes, and the gap between the lowest unoccupied molecular orbit (LUMO) and the highest occupied molecular orbit (HOMO), and thus the blue-shift is observed in the case of AlQ_3 incorporated into nanochannels of SBA-15. When the concentration of AlQ_3 complexes reaches a higher level, the interaction between AlQ_3 complexes gets increased and therefore the emission wavelength becomes longer (Badiei and Goldooz 2012; Badiei et al. 2011; Wang et al. 2006b).

Table 2 Emission peak maxima of AlQ_3-PMMA-*co*-PBuA nanoparticles at various concentrations of AlQ_3

Sample	%0.01-AlQ_3-poly	%0.1-AlQ_3-poly	%1-AlQ_3-poly	AlQ_3
Wavelength (nm)	447	466	507	507
Energy (eV)	2.77	2.66	2.45	2.45

Table 3 Emission peak maxima of AlQ_3, AlQ_3-SBA-15, Co-Poly-AlQ_3-SBA-15

Compounds	Emission (nm)
AlQ_3	507
AlQ_3-SBA-15	495
Co-Poly-AlQ_3-SBA-15[a]	460

[a] Co-Poly-AlQ_3-SBA-15 with different concentrations of AlQ_3-SBA-15

Figure 6 also shows the fluorescence emission spectra of Co-Poly-AlQ_3-SBA-15. It is clear from the emission spectra that there is a shift to shorter wavelength when AlQ_3-SBA-15 is incorporated into the PMMA-*co*-PBuA matrix by blending method. As discussed above, we assume that this blue-shifted behavior might be the result of the reduced polarity of the environment around AlQ_3 complexes.

It is interesting to see that the position of emission peak for Co-Poly-AlQ_3-SBA-15 showed independence on the AlQ_3-SBA-15 concentrations. Indeed, the maximum emission wavelength of Co-Poly-AlQ_3-SBA-15 is stable at various concentrations of AlQ_3-SBA-15. We hypothesized that due to the lack of molecular interactions between AlQ_3 molecules no change was observed in the fluorescence spectra. As can be seen from Fig. 7, it is reasonable to assume that there is physically room for only a limited number of AlQ_3 molecules per pore. Therefore, the AlQ_3 molecules are not only isolated inside the nanochannels of mesoporous silica, but also are individually embedded in a polymer matrix. Thus, encapsulation of AlQ_3-SBA-15 in the PMMA-*co*-PBuA matrix probably inhibits molecular interaction effects between AlQ_3 molecules, resulting in stable emission wavelength in different concentrations of AlQ_3-SBA-15 (Baldacchini et al. 2009; Tagaya and Ogawa 2008).

Conclusions

A new and simple method for studying environmental and concentration effects on luminescent properties of fluorophore was studied. To this end, AlQ_3 was chosen as one of the best reporter molecules due to its spectral sensitivity, ability to modify organic and inorganic materials and its potential application in fabricate photoelectric devices such as OLED. First AlQ_3 complexes were loaded into PMMA-*co*-PBuA nanoparticles as organic compounds with different weight percent of AlQ_3 by emulsion polymerization method. The results demonstrated that there is a blue-shift with decreasing concentration of AlQ_3. Generally, decreasing the aggregation of AlQ_3 complexes and the reduced polarity of the environment causes a blue-shift of emission bands. Another study was directed to the adsorption of AlQ_3 into the nanochannels of SBA-15 as an inorganic host material. Because of the strong steric confinement effect of the local environment, it is difficult for AlQ_3 to aggregate into the nanochannels of SBA-15. Thus the AlQ_3 complexes should be highly dispersed and present in diluted concentration resembling rather the monomers. The position of the maximum emission peak for these monomers shifts to the short wavelength region in comparison to pure AlQ_3. AlQ_3-functionalized SBA-15/polymer fluorescent composites (Co-Poly-AlQ_3-SBA-15) were

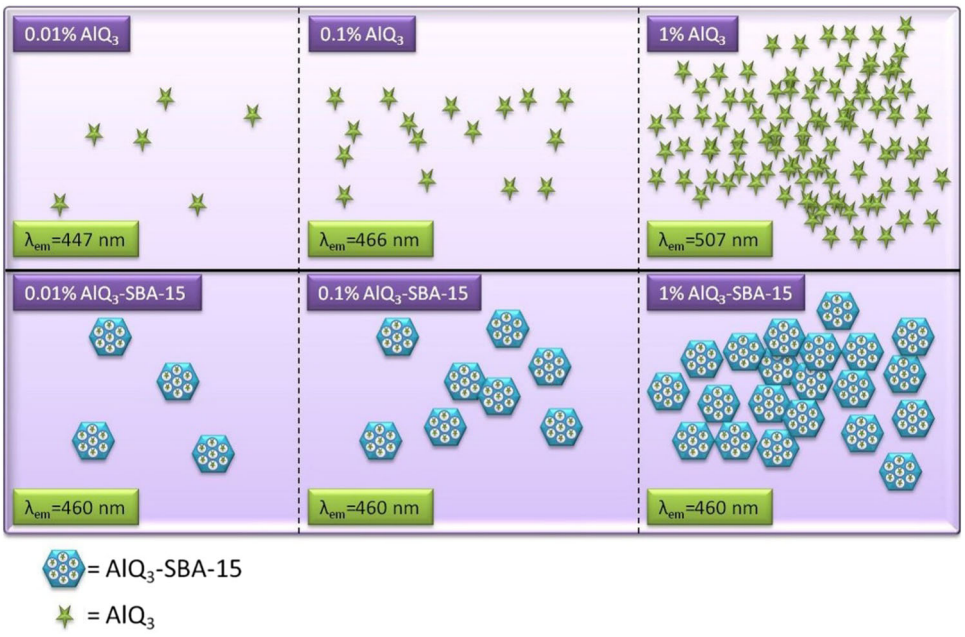

Fig. 7 Proposed schematic representation of how various concentrations of AlQ_3 and AlQ_3-SBA-15 guest compound may be accommodated into the PMMA-*co*-PBuA matrix

prepared by a blending method. The interaction between PMMA-*co*-PBuA matrix and AlQ_3-SBA-15 influences the emission spectra of the resulting composites. It was assumed that this shift to shorter wavelengths in the fluorescence spectra is related to the decrease in dielectric constant and polarity of the environment around AlQ_3 molecules. It is, however, interesting to note here that the maximum emission wavelength of Co-Poly-AlQ_3-SBA-15 is stable at various concentrations of AlQ_3-SBA-15. It was hypothesized that due to the lack of molecular interactions between AlQ_3 molecules no change was observed in the fluorescence spectra.

Acknowledgements The authors thank the University of Tehran for support of this work.

References

Antony R, Ratier B, Moliton A (1999) Realization of red light-emitting diodes with a confinement layer. Opt Mater 12:291–294. doi:10.1016/s0925-3467(99)00034-8

Auzel F, Baldacchini G, Baldacchini T, Chiacchiaretta P, Balaji Pode R (2006) Rayleigh scattering and luminescence blue shift in tris(8-hydroxyquinoline)aluminum films. J Lumin 119–120:111–115. doi:10.1016/j.jlumin.2005.12.018

Badiei A, Goldooz H (2012) A simple method for preparation of fluorescent nanostructure silica with hexagonal array. Int J Mod Phys Conf Ser 05:151–159. doi:10.1142/S2010194512001961

Badiei A, Goldooz H, Ziarani GM (2011) A novel method for preparation of 8-hydroxyquinoline functionalized mesoporous silica: aluminum complexes and photoluminescence studies. Appl Surf Sci 257:4912–4918. doi:10.1016/j.apsusc.2010.12.146

Balamurugan A, Kannan S, Selvaraj V, Rajeswari S (2004) Development and spectral characterization of poly(methyl methacrylate)/hydroxyapatite composite for biomedical applications. Trends Biomater Artif Organs 18:41–45

Baldacchini G, Chiacchiaretta P, Reisfeld R, Zigansky E (2009) The origin of luminescence blueshifts in Alq_3 composites. J Lumin 129:1849–1852. doi:10.1016/j.jlumin.2009.04.036

Bradley M, Ashokkumar M, Grieser F (2002) Sonochemical production of fluorescent and phosphorescent latex particles. J Am Chem Soc 125:525–529. doi:10.1021/ja0268581

Braun MGJ, Tzolov M, Coelle M, Meyer FD, Milius W, Hillebrecht H, Wendland O, von Schütz JU, Brütting W (2001) A new crystalline phase of the electroluminescent material tris(8-hydroxyquinoline) aluminum exhibiting blueshifted fluorescence. J Chem Phys 114:9625–9632. doi:10.1063/1.1369157

Brinkmann M, Gadret G, Muccini M, Taliani C, Masciocchi N, Sironi A (2000) Correlation between molecular packing and optical properties in different crystalline polymorphs and amorphous thin films of mer-tris(8-hydroxyquinoline)aluminum(III). J Am Chem Soc 122:5147–5157. doi:10.1021/ja993608k

Cölle M, Brütting W (2004) Thermal, structural and photophysical properties of the organic semiconductor Alq_3. Phys Status Sol (a) 201:1095–1115. doi:10.1002/pssa.200404341

Cölle M, Gmeiner J, Milius W, Hillebrecht H, Brütting W (2003) Preparation and characterization of blue-luminescent tris(8-hydroxyquinoline)aluminum (Alq_3). Adv Func Mater 13:108–112. doi:10.1002/adfm.200390015

Curry RJ, Gillin WP, Clarkson J, Batchelder DN (2002) Morphological study of aluminum tris(8-hydroxyquinoline) thin films using infrared and Raman spectroscopy. J Appl Phys 92:1902. doi:10.1063/1.1495527

Deshmukh RR, Arolkar GA, Parab SS (2012) Studies in dielectric properties of various polymers and its correlation with surface free energy. Int J Chem Phys Sci 1:40–47

Du Y, Fu Y, Guo X, Li H, Lü C, Su Z (2010) Fabrication of fluorescent mesoporous silica nanoparticles with confined 8-hydroxyquinoline functionalized ZnS nanoparticles and their transparent polymer nanocomposites. Microporous Mesoporous Mater 130:122–129. doi:10.1016/j.micromeso.2009.10.022

Ganjali MR, Gupta VK, Hosseini M, Rafiei-Sarmazdeh Z, Faridbod F, Goldooz H, Badiei AR, Norouzi P (2012) A novel permanganate-sensitive fluorescent nano-chemosensor assembled with a new 8-hydroxyquinoline-functionalized SBA-15. Talanta 88:684–688. doi:10.1016/j.talanta.2011.11.065

Hashemi P, Shamizadeh M, Badiei A, Poor PZ, Ghiasvand AR, Yarahmadi A (2009) Amino ethyl-functionalized nanoporous silica as a novel fiber coating for solid-phase microextraction. Anal Chim Acta 646:1–5. doi:10.1016/j.aca.2009.04.023

Hoffmann F, Cornelius M, Morell J, Fröba M (2006) Silica-based mesoporous organic–inorganic hybrid materials. Angew Chem Int Ed 45:3216–3251. doi:10.1002/anie.200503075

Karimi M, Badiei A, Mohammadi Ziarani G (2015a) A single hybrid optical sensor based on nanoporous silica type SBA-15 for detection of Pb^{2+} and I^- in aqueous media. RSC Adv 5:36530–36539. doi:10.1039/c5ra02692j

Karimi M, Badiei A, Lashgari N, Afshani J, Mohammadi Ziarani G (2015b) A nanostructured LUS-1 based organic–inorganic hybrid optical sensor for highly selective sensing of Fe^{3+} in water. J Lumin 168:1–6. doi:10.1016/j.jlumin.2015.07.007

Kruk M, Dufour B, Celer EB, Kowalewski T, Jaroniec M, Matyjaszewski K (2008) Grafting monodisperse polymer chains from concave surfaces of ordered mesoporous silicas. Macromolecules 41:8584–8591. doi:10.1021/ma801643r

Kushto GP, Iizumi Y, Kido J, Kafafi ZH (2000) A matrix-isolation spectroscopic and theoretical investigation of tris(8-hydroxyquinolinato)aluminum(iii) and tris(4-methyl-8-hydroxyquinolinato)aluminum(iii). J Phys Chem A 104:3670–3680. doi:10.1021/jp993883t

Lee Y, Kim J, Kwon S, Min C-K, Yi Y, Kim JW, Koo B, Hong M (2008) Interface studies of Aluminum, 8-hydroxyquinolatolithium (Liq) and Alq_3 for inverted OLED application. Org Electron 9:407–412. doi:10.1016/j.orgel.2008.01.001

Levichkova MM, Assa JJ, Fröb H, Leo K (2006) Blue luminescent isolated Alq_3 molecules in a solid-state matrix. Appl Phys Lett 88:201912. doi:10.1063/1.2203966

Li Y-J, Yan B (2009) Lanthanide (Eu^{3+}, Tb^{3+})/β-diketone modified mesoporous SBA-15/organic polymer hybrids: chemically bonded construction, physical characterization, and photophysical properties. Inorg Chem 48:8276–8285. doi:10.1021/ic900971h

Li N, Li X, Wang W, Geng W, Qiu S (2006) Blue-shifting photoluminescence of Tris(8-hydroxyquinoline) aluminium encapsulated in the channel of functionalized mesoporous silica SBA-15. Mater Chem Phys 100:128–131. doi:10.1016/j.matchemphys.2005.12.020

Magee RJ, Gordon L (1963) The infrared spectra of chelate compounds—I: a study of some metal chelate compounds of 8-hydroxyquinoline in the region 625–5000 cm^{-1}. Talanta 10:851–859. doi:10.1016/0039-9140(63)80245-3

Mahakhode JG, Dhoble SJ, Joshi CP, Moharil SV (2011) Blue-shifted photoluminescence of Alq_3 dispersed in PMMA. Bull Mater Sci 34:1649–1651

Meyers A, Weck M (2003) Design and synthesis of Alq_3-functionalized polymers. Macromolecules 36:1766–1768. doi:10.1007/s12034-011-0372-1

Nakamoto K, Ohkaku N (1971) Metal isotope effect on metal-ligand vibrations. VI. Metal complexes of 8-hydroxyquinoline. Inorg Chem 10:798–805. doi:10.1021/ic50098a027

Park JH, Kim S, Kim YC, Park OO (2005) Polymer/nanoporous silica nanocomposite blue-light-emitting diodes. Nanotechnology 16:1793–1797

Poostforooshan J, Rennecke S, Gensch M, Beuermann S, Brunotte G-P, Ziegmann G, Weber AP (2014) Aerosol process for the in situ coating of nanoparticles with a polymer shell. Aerosol Sci Technol 48:1111–1122. doi:10.1080/02786826.2014.964354

Poostforooshan J, Badiei A, Kolahdouz M, Weber AP (2016) Synthesis of spherical carbon nitride-based polymer composites by continuous aerosol–photopolymerization with efficient light harvesting. ACS Appl Mater Interfaces 8:21731–21741. doi:10.1021/acsami.6b07909

Scott BJ, Wirnsberger G, Stucky GD (2001) Mesoporous and mesostructured materials for optical applications. Chem Mater 13:3140–3150. doi:10.1021/cm0110730

Shaban M, Ramazani SAA, Ahadian MM, Tamsilian Y, Weber AP (2016) Facile synthesis of cauliflower-like hydrophobically modified polyacrylamide nanospheres by aerosol-photopolymerization. Eur Polymer J 83:323–336. doi:10.1016/j.eurpolymj.2016.08.022

Shahbazi A, Younesi H, Badiei A (2011) Functionalized SBA-15 mesoporous silica by melamine-based dendrimer amines for adsorptive characteristics of Pb(II), Cu(II) and Cd(II) heavy metal ions in batch and fixed bed column. Chem Eng J 168:505–518. doi:10.1016/j.cej.2010.11.053

Tagaya M, Ogawa M (2008) Possible pore size effects on the state of tris(8-quinolinato)aluminum(iii) (Alq_3) adsorbed in mesoporous silicas and their temperature dependence. Phys Chem Chem Phys 10:6849–6855. doi:10.1039/B807593J

Tang CW, VanSlyke SA (1987) Organic electroluminescent diodes. Appl Phys Lett 51:913–915. doi:10.1063/1.98799

Wang H, Huang J, Wu S, Xu C, Xing L, Xu L, Kan Q (2006a) Design and synthesis of Alq_3-functionalized SBA-15 mesoporous material. Mater Lett 60:2662–2665. doi:10.1016/j.matlet.2006.01.059

Wang H, Huang J, Wu S, Xu C, Xing L, Xu L, Kan Q (2006b) Design and synthesis of Alq_3-functionalized SBA-15 mesoporous material. Mater Lett 60:2662–2665. doi:10.1016/j.matlet.2006.01.059

Wang X, Xu S, Xu W (2011a) Luminescent properties of dye-PMMA composite nanospheres. Phys Chem Chem Phys 13:1560–1567. doi:10.1039/c0cp00929f

Wang X, Xu S, Liang C, Li H, Sun F, Xu W (2011b) Enriching PMMA nanospheres with adjustable charges as novel templates for multicolored dye@PMMA nanocomposites. Nanotechnology 22:275608

Wei L, Hu N, Zhang Y (2010) Synthesis of polymer-mesoporous silica nanocomposites. Materials 3:4066–4079

Zhang F-A, Lee D-K, Pinnavaia TJ (2010) PMMA/mesoporous silica nanocomposites: effect of framework structure and pore size on thermomechanical properties. Polymer Chemistry 1:107–113. doi:10.1039/b9py00232d

Zhao D, Huo Q, Feng J, Chmelka BF, Stucky GD (1998) Nonionic triblock and star diblock copolymer and oligomeric surfactant syntheses of highly ordered, hydrothermally stable, mesoporous silica structures. J Am Chem Soc 120:6024–6036. doi:10.1021/ja974025i

Zou H, Wu S, Shen J (2008) Polymer/silica nanocomposites: preparation, characterization, properties, and applications. Chem Rev 108:3893–3957. doi:10.1021/cr068035q